J Fluoresc (2015) 25:311–317
DOI 10.1007/s10895-015-1510-8

ORIGINAL PAPER

Metal-Enhanced Fluorescence of Dye-Doped Silica Nano Particles

Kalani B. Gunawardana · Nathaniel S. Green · Lloyd A. Bumm · Ronald L. Halterman

Received: 9 September 2014 / Accepted: 4 January 2015 / Published online: 28 January 2015

Abstract Recent advancements in metal-enhanced fluorescence (MEF) suggest that it can be a promising tool for detecting molecules at very low concentrations when a fluorophore is fixed near the surface of metal nanoparticles. We report a simple method for aggregating multiple gold nanoparticles (GNPs) on Rhodamine B (RhB)-doped silica nanoparticles (SiNPs) utilizing dithiocarbamate (DTC) chemistry to produce MEF in solution. Dye was covalently incorporated into the growing silica framework via co-condensation of a 3-aminopropyltriethoxysilane (APTES) coupled RhB precursor using the Stöber method. Electron microscopy imaging revealed that these mainly non-spherical particles were relatively large (80 nm on average) and not well defined. Spherical core-shell particles were prepared by physisorbing a layer of RhB around a small spherical silica particle (13 nm) before condensing an outer layer of silica onto the surface. The core-shell method produced nanospheres (~30 nm) that were well defined and monodispersed. Both dye-doped SiNPs were functionalized with pendant amines that readily reacted with carbon disulfide (CS_2) under basic conditions to produce DTC ligands that have exhibited a high affinity for gold surfaces. GNPs were produced via citrate reduction method and the resulting 13 nm gold nanospheres were then recoated with an ether-terminated alkanethiol to provide stability in ethanol. Fluorescent enhancement was observed when excess GNPs were added to DTC coated dye-doped SiNPs to form nanoparticle aggregates. Optimization of this system gave a fluorescence brightness enhancement of over 200 fold. Samples that gave fluorescence enhancement were characterized through Transmission Emission Micrograph (TEM) to reveal a pattern of multiple aggregation of GNPs on the dye-doped SiNPs.

Keywords Metal-enhanced fluorescence · Gold nanoparticles · Silica nanoparticles · Nanoparticle aggregation

Enhancement of molecular fluorescence is of great interest due to the widespread and evolving utility of fluorescence-based detection techniques [1–3]. The sensitivity of such detection is dependent on inherent fluorophore brightness and stability [4, 5]. Although fluorescence-based detection is considered to be more sensitive than other optical approaches there is still a need for the development of more photo stable, high quantum yield fluorophores, which would greatly enhance the effectiveness of techniques in single molecule detection [6, 7], cellular tracking and imaging [8], as well as the miniaturization of optical sensors [9, 10].

Metal-enhanced fluorescence (MEF) is a powerful technique that simultaneously increases photo stability and brightness of fluorescent molecules [9, 11–14]. MEF originates due to near field interactions (within a wavelength of light) of surface plasmon resonance (SPR) of metal colloids with fluorophores [7]. This effect is highly sensitive to the distance between the nanoparticle and the fluorophore (~5–30 nm) [15]. Furthermore, MEF can be influenced by the size, shape, and aggregation of the metal particles as well as the spectral overlap of the SPR with the absorbance and emission bands of the fluorophore [16–20]. In particular, it has been shown both theoretically [19–23] and experimentally, that the overlap of

Electronic supplementary material The online version of this article (doi:10.1007/s10895-015-1510-8) contains supplementary material, which is available to authorized users.

K. B. Gunawardana (✉) · N. S. Green · R. L. Halterman
Department of Chemistry and Biochemistry, University of Oklahoma, Norman, OK 73019-5251, USA
e-mail: kalanigunawardana@gmail.com

L. A. Bumm
Homer L. Dodge Department of Physics and Astronomy, University of Oklahoma, Norman, OK 73019-5251, USA

multiple plasmons of nearby metal colloids would strongly intensify the electromagnetic field in the overlapped region and a single fluorophore located in this region has shown greater brightness enhancements [24–27]. Enhancements greater than 50 fold have been reported for fluorophores next to multiple silver nanoparticles with large scattering cross sections [19]. However, these MEF techniques required stationary immobilization or bio-molecule tethering that are most practical for surface assays [26]. One of the few studies carried out in a solution–based sensing platform using metal-fluorophore aggregation showed that silica-coated silver colloids labeled with Cy3 gave a 3–5 fold enhancement of fluorescence [27]. These models demonstrate an ability to achieve massive MEF levels and point out a need to enable wider MEF applications using a more general solution-based aggregation method [27–29].

In this work we report a simple solution-based approach for aggregating multiple gold nanoparticles (GNPs) around Rhodamine B (RhB)-doped silica nanoparticles (SiNPs) using dithiocarbamate (DTC) attachment. We aimed to achieve large enhancement factors by placing a fluorophore at the optimal distance from the gold surface as well as aggregating multiple gold nanoparticles around a small number of dye molecules. We have used dye-doped SiNPs as solution-suspended fluorescent nano-platforms. The silica framework allowed for a fixed distance to be created between the dyes and metallic surface and provided a platform for multiple GNPs to be attached in solution. The resulting extremely bright metal-fluorophore aggregates support a greater potential of creating MEF using solution-based methods.

Materials and Methods

For this study dye-doped SiNPs were produced by two methods as fully detailed in the Supplementary Material. In method 1, modified Stöber method was used to prepare dye-doped SiNPs. Initially, RhB dye was covalently attached to an APTES-derived siloxane tether by reacting RhB (0.100 g, 0.2 mmol), 1-(3-dimethylaminopropyl)-3-ethylcarbodiimide hydrochloride (EDC) (0.080 g, 0.40 mmol), n-hydroxysuccinimide (NHS) (0.050 g, 0.40 mmol), 4-dimethylaminopyridine (DMAP) (0.005 g, 0.040 mmol) in dimethylformamide (DMF) (5 mL) for 12 h, followed by addition of APTES (94.7 μL, 0.40 mmol) under nitrogen atmosphere for 24 h in the dark. SiNPs were produced by co-condensing the siloxane-tethered RhB units (1.5 mL in DMF) with tertaethoxyorthosilicate (TEOS) (0.335 mL) in a 0.06:1.5 molar ratio in the presence of pure ethanol (8.75 mL) and ammonium hydroxide (NH_4OH), (0.64 mL) for 24 h [30]. Two batches of dye doped SiNPs with different dye concentrations were produced by Stöber method. Particles doped with high concentration of dye were produced by mixing siloxane-tethered RhB units with NH_4OH for 12 h prior addition of TEOS. Particles doped with low concentration of dye were produced by mixing the above two components for 5 min prior addition of TEOS. This co-condensation method produced amorphous particles that presumably contained RhB dye dispersed throughout the SiNP [31]. Based on the mass balance of these condensation reactions, we could estimate the concentration of the silica particles in stock aqueous suspensions. We examined these SiNPs by transmission electron microscopy (TEM) to determine that they were amorphous particles with a cross section of 100 nm. TEM imaging was performed on a Zeiss 10A Conventional microscope operating at 80 kV from a tungsten filament source at the University of Oklahoma Samuel Roberts Noble Electron Microscopy Laboratory. Samples were prepared by drop coating 4 μL of sample onto a 300 mesh formvar coated copper TEM grid (Ted Pella Corp.) and allowing to dry under ambient air.

In Method 2, a core-shell design was used to hold the dye at a set distance from the metal surface by sandwiching layer of dye between two concentric spheres of silica [32]. The two types of dye-doped SiNPs are illustrated in Fig. 1. Layered SiNP were prepared to control both the size of the spheres and the location of flourophore within the silica matrix. TEM imaging confirmed the production of 16 nm spherical SiNPs.

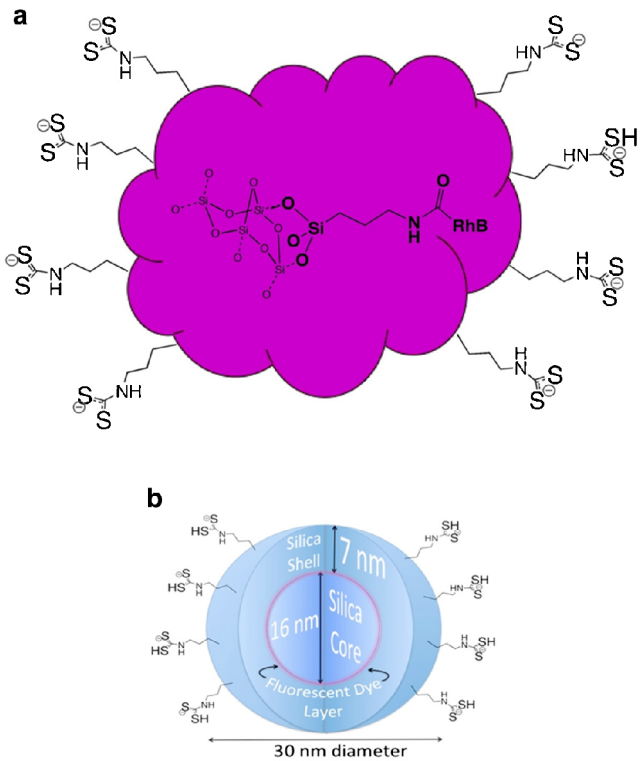

Fig. 1 Two motifs for RhB incorporation into silica nanoparticles. **a** Amorphous particles with covalent dye attachment throughout the entire SiNP via 3-aminopropyltriethoxysilane (APTES) bound RhB. **b** Spherical particles with RhB dye shell formed by physisorption in layered silica preparation

Cationic RhB dye was then physisorbed in an aqueous suspension onto the surface of these well-defined core particles [32]. Finally, an additional layer of silica was grown by a lysine catalyzed condensation of TEOS in an aqueous organic biphasic system to provide an outer shell for small diameter layered SiNPs. The dye-doped particles were purified by membrane dialysis (12–14 kD MWCO) against milipore water. Dye loading was found to be 95 % based on the absorbance of the dialysis water to determine the amount of fluorophore that was not incorporated. TEM imaging confirmed the formation of monodisperse 30 nm SiNPs. The optical absorption and emission spectra of both stock SiNP mixtures produced by the two different methods were measured. Absorbance measurements were taken on a Shimadzu Scientific UV-2101 PC UV–Vis scanning spectrophotometer. Fluorescence measurements were taken on a Shimadzu Scientific RF-5301 PC spectrofluorophotometer equipped with a xenon lamp of 150 W as an excitation source.

Gold nanoparticles were produced via the well-established reduction of chloroauric acid in aqueous sodium citrate [33, 34]. The resulting citrate-stabilized 13 nm gold nanospheres were then recoated with (10-(2-(2-methoxyethoxy)ethoxy)decane-1-thiol $CH_3O(CH_2CH_2O)2C_{10}H_{20}SH$), an ether-terminated alkanethiol to provide stability in water/ethanol mixture. For this surface funtionalization, S-10-[2-(2 methoxyethoxy)ethoxy] decyl ethanethioate ($CH_3O(CH_2CH_2O)C_{10}H_{20}SOCH_3$) was synthesized [35]. GNPs were capped with $CH_3O(CH_2CH_2O)2C_{10}H_{20}SH$ by ligand exchange after cleavage of thioacetate group [36]. Recoating of GNPs with the ether-terminated alkanethiol was optically characterized by the slight red shifting of the 520 nm UV/Vis spectra of the GNP plasmon. The concentration of the stock GNP solution was then estimated using the extinction coefficient [37, 38].

Establishing a robust method for attaching gold and silica particles together is vital to optimizing MEF as the enhancement factor rises with increased aggregation. Wie et al. have demonstrated that dithiocarbamate (DTC) effectively stabilizes ligands on gold surfaces [39]. Recently, DTC chemistry has been used to immobilize gold nanoparticles on amine coated bulk silica substrates [40]. This method was modified to covalently bind SiNPs to GNPs in solution (Fig. 2). For DTC activation, the surface of the SiNPs were amino funtionalized and then mixed with CS_2 under basic conditions. Particles produced by the modified Stöber method were initially used for DTC activation. For amino-propyl surface functionalization, RhB doped SiNPs (50 mg) were mixed with glacial acetic acid (100 μL) and APTES (100 μL) in deionized water (5 mL) and stirred for 4 h at room temperature. The reaction was quenched by centrifugation and the particles were washed and vacuum dried. A stock solution (1.2 mg/mL, 4.2 nM) was prepared by dissolving amino-propyl functionalized SiNPs in deionized water. Particles were DTC activated by adding varying amounts of amino-propyl functionalized SiNPs (250, 25, 12.5, 10 μL) to CS_2 solutions (1 mM, 3 mL) prepared in 95 % ethanol. The pH of the samples was raised to 9.8 by drop-wise addition of concentrated KOH and the samples were stirred for 30 min to complete DTC activation in capped glass vials. For nano particle aggregation, ether-terminated alkanethiol capped GNPs (1.0 mL, 1.2 nM) were added to the DTC-activated SiNP mixtures and stirring was continued for another 24 h. Above SiNP and GNP amounts were chosen to approximately provide desired SiNP to GNP ratios to be 1:1, 1:10 and 1:20, absorbance and emission of the samples were measured over time. Enhancement was measured by comparing the emission spectra of RhB-doped SiNP control samples that lacked GNPs. The amount of aggregation was compared relative to absorption spectra of SiNP and GNP mixtures lacking CS_2 so that DTC formation was prohibited. Once the amount of SiNPs that exhibited enhancement was screened, enhancement was further optimized by varying the GNP concentration. Experiment was repeated with SiNPs having high and low concentrations of dye loadings produced by the Stöber method.

Layered dye-doped SiNPs produced by Method 2 were similarly treated. However, the concentration of the stock solution of the layered particles was difficult to obtain as these particles did not efficiently centrifuge out of solution. Therefore, an aliquot that provided the same fluorescence emission as in method 1 was used. The same procedure described for method 1 was used for APTES coating and DTC activation of

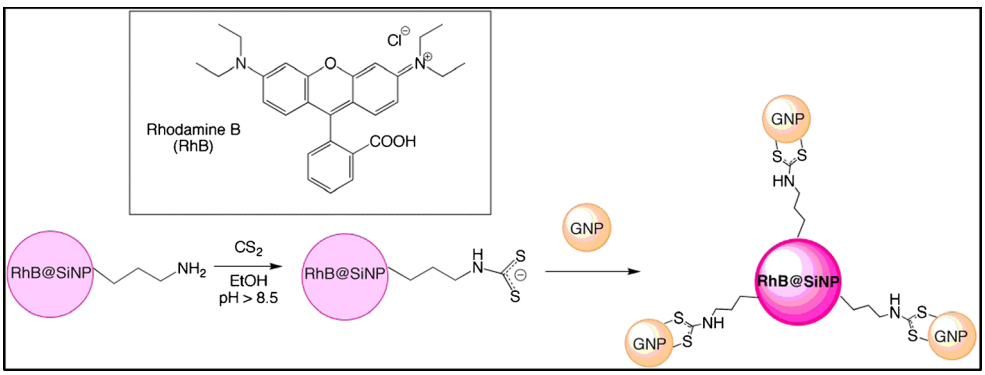

Fig. 2 Conversion of amino-propyl coated silica nanoparticles to dithiocarbamate (DTC) thus, promoting aggregation with gold nanoparticles

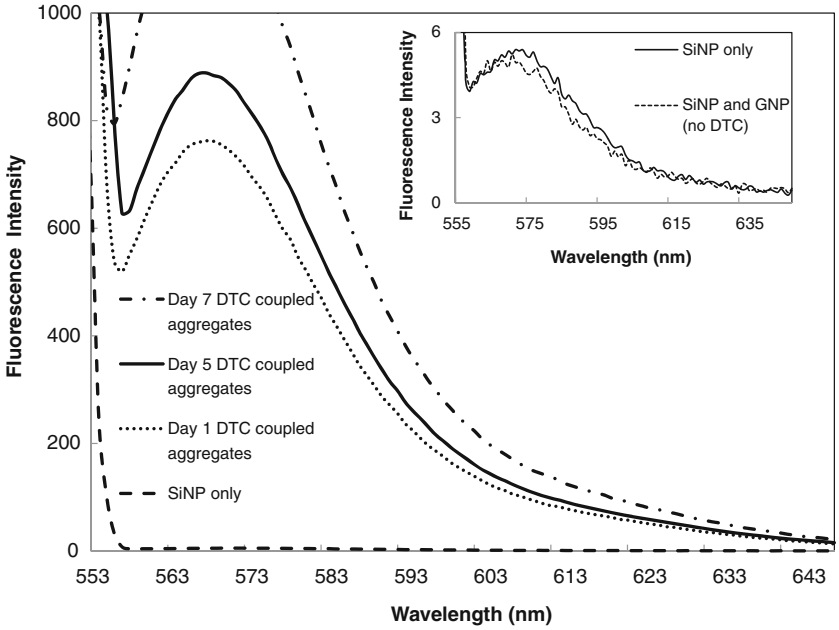

Fig. 3 Emission spectra of DTC activated RhB-doped silica nanoparticles mixed with gold nanoparticles over the course of 7 days. Inset shows the emission spectra of control samples

layered SiNPs. 30 min after DTC activation, ether-terminated alkanethiol capped GNPs (0.5 mL) were added and the samples were mixed continuously to form metal-fluorophore aggregates. The absorbance and emission were measured over time. Enhanced samples of metal-fluorophore aggregates formed by SiNPs from method 1 and method 2 were imaged through TEM to study the aggregation pattern.

Results and Discussion

Dye-doped SiNPs produced by two methods were interacted with GNPs to study MEF. The size of the silica nanoparticles was controlled by the amount of catalytic base added to the Stöber preparation or by the number of silica coatings added in the core-shell preparation. Gold nanoparticles size was also easily controlled by the amount of sodium citrate added to the aqueous reduction mixture. Re-coating of GNPs with ether-terminated alkanethiol provided stability in water/ethanol mixture. These particles were monodispersed and showed excellent colloidal stability in solution as evidenced by TEM. Calculating the concentration of GNPs was easily performed by calculations from absorbance measurements. Concentration of the SiNPs produced by the Stöber method was estimated based on the mass balance of these condensation reactions of the aqueous suspensions. Unfortunately, the same could not be done for the layered dye-doped SiNPs. The relative amount of dye molecules absorbed into a sphere could be estimated but extending this approximation to estimating the concentration of SiNP proved unhelpful. Both Stöber and layered particles were initially functionalized with the amino-propyl ligands that were subsequently converted to DTC by reaction of CS_2 under basic conditions. Ether-terminated alkanethiol capped GNPs were then added to DTC activated dye-doped SiNPs to produce metal-fluorophore aggregates. Both SiNP species showed GNP aggregation, which lead to large enhancements in fluorescent brightness [41, 42].

To achieve fluorescent enhancement it was necessary to optimize the concentrations of the dye-doped SiNPs and GNPs as well as establish a robust aggregation motif. Using dye-doped SiNPs produced by Method 1, different ratios of ether-terminated alkanethiol capped GNPs were mixed with DTC activated SiNPs in water/ethanol mixture to form metal-fluorophore aggregates. The fluorescence and absorbance of the mixtures were measured over time. Optical enhancement of experimental samples was relative to the fluorescence emission of SiNPs in the absence of GNPs. The aggregation of the nanoparticles mixtures due to DTC activation was determined by monitoring the red shifting of the absorbance spectra as an indication of interacting GNPs [43]. The enhancement process

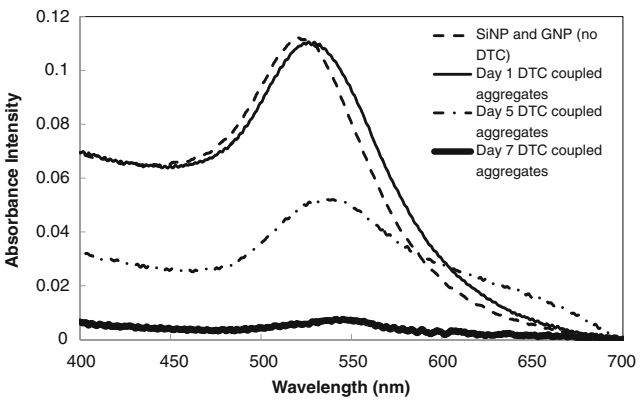

Fig. 4 Absorption spectra of DTC activated RhB-doped silica nanoparticles mixed with gold nanoparticles over the course of 7 days

proved to be very sensitive to the ratio of SiNPs to GNPs. While no enhancement was observed when GNPs and Method 1 SiNPs were mixed at a 1:1 ratio (see Figure S1), an increase in fluorescent brightness at higher GNP concentrations was observed (see Figure S2, S3). A significant increase in enhancement was also observed when the concentration of RhB dye was lowered within the SiNPs. This result is consistent with a reduction of fluorophore auto quenching that is observed for highly concentrated samples of RhB [44]. The fluorescence enhancement of these particles varied over time, increasing from about 100 fold after the first day to 200 fold after 7 days (Fig. 3). The absorbance spectra also red shifted (Fig. 4) as the fluorescence continued to increase over time. The increased red shift is consistent with increased GNP aggregation. A variation in the aggregation of GNPs around the amorphous dye-doped SiNPs was studied by TEM imaging.

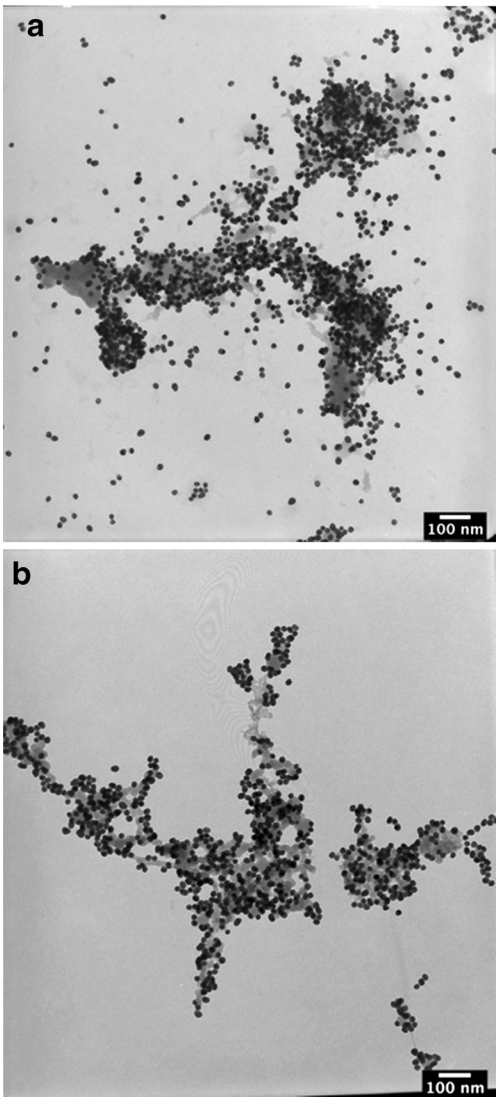

Fig. 5 TEM micrographs of gold nanoparticle and RhB-doped, DTC activated silica nanoparticle mixtures; **a** 2 days **b** 14 days after mixing

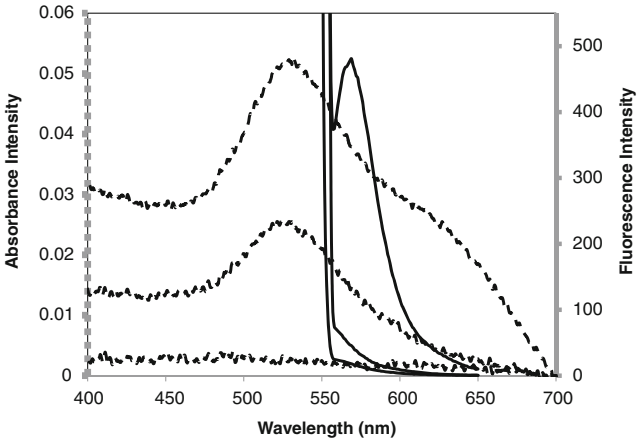

Fig. 6 (*Top*) Absorbance (*dotted line*) and emission (*solid line*) spectra of DTC activated RhB-doped layered SiNP mixed with GNP after 1 day. (*Bottom*) Absorbance (*dotted line*), emission (*solid lines*) spectra of non-DTC functionalized RhB-doped layered SiNP mixed with GNP after 1 day and emission spectra of RhB-doped layered SiNPs

TEM studies of these samples show an increasing degree of SiNP/GNP aggregation over the course of several days (Fig. 5). These images are in excellent agreement with the observed extinction spectra that show a gradual decrease in gold plasmon absorption (Fig. 4) as the amount of colloidal gold decreases. This supports the theory that fluorescent enhancement is due to GNP aggregation, which leads to increased plasmonic scattering [45, 46].

Treatment of the layered dye-doped SiNPs produced by method 2 was similarly studied. GNP aggregation was once again demonstrated concurrently with the increased emission (Fig. 6). Formation of aggregates was confirmed by red shifting of the absorbance spectra, the emission spectra showed about 50-fold enhancement on day 1 and about 100-fold enhancement after 8 days (see Figure S8). TEM images of these samples further confirmed formation of metal-fluorophore aggregates.

One limitation of this solution-based approach is the difficulty in controlling the aggregation in solution phase. It was difficult to reproduce the same amount of metal-fluorophore aggregation in each trial due to the inherent randomness associated with solution-based complexation. Thus, it was difficult to reproduce the fluorescence enhancement to the same level in each trial. However, we were able to reproduce enhancement in different amounts in several trials (see Figure S7).

Conclusion

In this study we have described a simple solution based approach to achieve metal-enhanced fluorescence by aggregation of a large concentration of gold nanoparticles around a smaller concentration of RhB doped silica nanoparticles. RhB doped SiNPs were produced by two methods; the first method

formed larger amorphous particles having dye throughout and the second method yielded smaller, more spherical particles having RhB dye sandwiched between two layers of silica. GNPs were coated with an ether-terminated alkanethiol to gain stability in water/ethanol mixture. Surface of dye-doped SiNPs were DTC activated and mixed with GNPs in water/ethanol solutions to form metal-fluorophore aggregates. Absorbance spectra confirmed that both kinds of SiNPs showed metal-fluorophore aggregation and the aggregation increased over time. We achieved 100-fold fluorescence enhancement on the first day, which increased up to 200 fold over period of 7 days. TEM data was used to further confirm metal-fluorophore aggregation. This novel technique allows the study of MEF by a simple solution based approach using SiNPs as fluorescent nano platforms. Employment of DTC chemistry for metal fluorophore aggregation simplifies the need for biomolecule tethering in study of MEF. Further work on learning to better control the degree of aggregation is now needed to better harness this very powerful MEF effect.

Acknowledgments We thank the NSF for funding this work (DMR – 0805233). We thank Anuradha Singh for providing S-10-[2-(2 methoxyethoxy)ethoxy]decyl ethanethioate ($CH_3O(CH_2CH_2O)C_{10}H_{20}SOCH_3$) for GNP surface functionalization.

References

1. Drummen GPC (2012) Fluorescent probes and fluorescence (Microscopy) techniques — illuminating biological and biomedical research. Molecules 17(12):14067–14090
2. Lakowicz JR (2006) Plasmonics in biology and plasmon-controlled fluorescence. Plasmonics 1(1):5–33
3. Anker JN, Hall WP, Lyandres O, Shah NC, Zhao J, van Duyne RP (2008) Biosensing with plasmonic nanosensors. Nat Mater 7(6):442–453
4. Aslan K, Lakowicz JR, Geddes CD (2005) Plasmon light scattering in biology and medicine: new sensing approaches, visions and perspectives. Curr Opin Chem Biol 9(5):538–544
5. Lakowicz JR (1999) Principles of Fluorescent Spectroscopy, 2nd edn. Springer, New York, p 725
6. Punj D, de Torres J, Rigneault H, Wenger J (2013) Gold nanoparticles for enhanced single molecule fluorescence analysis at micromolar concentration. Opt Express 21(22):27338–27343
7. Kühn S, Håkanson U, Rogobete L, Sandoghdar V (2006) Enhancement of single-molecule fluorescence using a gold nanoparticle as an optical nanoantenna. Phys Rev Lett 97(1):017402
8. Butler SJ, Lamarque L, Pal R, Parker D (2014) Eurotracker dyes: highly emissive europium complexes as alternative organelle stains for live cell imaging. Chem Sci 5:1750–1756
9. Geddes CD, Gryczynski I, Malicka J, Gryczynski Z, Lakowicz JR (2003) Metal-enhanced fluorescence: potential applications in HTS. Comb Chem High Throughput Screen 6(2):109–117
10. Jain PK, Huang X, El-Sayed IE, El-Sayed MA (2008) Nobel metals on the nanoscale: optical and photothermal properties and same applications in imaging, sensing, biology, and medicine. Acc Chem Res 41(12):1578–1586
11. Lakowicz JR, Ray K, Chowdhury M, Szmacinski H, Fu Y, Zhang J, Nowaczyk K (2008) Plasmon-controlled fluorescence: a new paradigm in fluorescence spectroscopy. Analyst 133:1308–1346
12. Aslan K, Gryczynski I, Malicka J, Matveeva E, Lakowicz JR, Geddes CD (2005) Metal-enhanced fluorescence: an emerging tool in biotechnology. Curr Opin Biotechnol 16(1):55–62
13. Zhang J, Lakowicz JR (2007) Metal-enhanced fluorescence of an organic fluorophore using gold particles. Opt Express 15(5):2598
14. Geddes CD, Lakowicz JR (2002) Metal-enhanced fluorescence. J Fluoresc 12(2):121–130
15. Dragan AI, Bishop ES, Casas-Finet JR, Strouse RJ, McGivney J, Schenerman MA, Geddes CD (2012) Distance dependence of metal-enhanced fluorescence. Plasmonics 7:739–744
16. Liu J, Li A, Tang J, Wang R, Kong N, Davis TP (2012) Thermoresponsive silver/polymer nanohybrids with switchable metal enhanced fluorescence. Chem Commun 48:4680–4682
17. Tam F, Goodrich GP, Johnson BR, Halas NJ (2007) Plasmonic enhancement of molecular fluorescence. Nano Lett 7(2):496–501
18. Zhang Y, Dragan A, Geddes CD (2009) Wavelength dependence of metal-enhanced fluorescence. J Phys Chem C 113(28):12095–12100
19. Zhang J, Fu Y, Chowdhury MH, Lakowicz JR (2008) Single-molecule studies on fluorescently labeled silver particles: effects of particle size. J Phys Chem C 112:18–26
20. Kelly LE, Coronado E, Zhao LL, Schatz GC (2003) The optical properties of metal nanoparticles: the influence of size, shape, and dielectric environment. J Phys Chem B 107(3):668–677
21. Quinten M, Leitner A, Krenn J, Aussenegg F (1998) Electromagnetic energy transport via linear chains of silver nanoparticles. Opt Lett 23(17):1331–1333
22. Hao E, Schatz GC (2004) Electromagnetic fields around silver nanoparticles and dimers. J Chem Phys 120:357
23. Su KH, Wei QH, Zhang X, Mock J, Smith D, Schultz S (2003) Interparticle coupling effects on plasmon resonances of nanogold particles. Nano Lett 3(8):1087–1090
24. Zhang J, Fu Y, Chowdhury MH, Lakowicz JR (2007) Metal-enhanced single-molecule fluorescence on silver particle monomer and dimer: coupling effect between metal particles. Nano Lett 7(7):2101–2107
25. Acuna GP, Moller FM, Holzmeister P, Beater S, Lalkens B, Tinnefeld P (2012) Fluorescence enhancement at docking sites of DNA-directed self-assembled nanoantennas. Science 338:506–510
26. Pan S, Wang Z, Rothberg LJ (2006) Enhancement of adsorbed dye monolayer fluorescence by a silver nanoparticle overlayer. J Phys Chem B 110:1783–17387
27. Aslan K, Lakowicz JR, Szmacinski H, Geddes CD (2004) Metal-enhanced fluorescence solution-based sensing platform. J Fluoresc 14(6):677–679
28. Aslan K, Wu M, Lakowicz JR, Geddes CD (2007) Fluorescent core-shell Ag@ SiO2 nanocomposites for metal-enhanced fluorescence and single nanoparticle sensing platforms. J Am Chem Soc 129(6):1524–1525
29. Furtaw MD, Lin D, Wu L, Anderson JP (2009) Near-infrared metal-enhanced fluorescence using a liquid–liquid droplet micromixer in a disposable poly (Methyl Methacrylate) microchip. Plasmonics 4(4):273–280
30. Wang L, Tan W (2006) Multicolor FRET silica nanoparticles by single wavelength excitation. Nano Lett 6(1):84–88
31. Ma D, Tan S, Jakubek ZJ, Simard B (2009) On the Structural Stability of Dye-Doped Silica Nanoparticles. IEEE Nano:651–655
32. Hartlen K, Athanasopoulos A, Kitaev V (2008) Facile preparation of highly monodisperse small silica spheres (15 to >200 nm) suitable for colloidal templating and formation of ordered arrays. Langmuir 24:1714–1720
33. Frens G (1972) Controlled nucleation for the regulation of the particle size in monodisperse gold suspensions. Nature Phys Sci 241:20–22

34. Polte J, Ahner TT, Delissen F, Sokolov S, Emmerling F, Thunemann AF, Kraehnert R (2010) Mechanism of gold nanoparticle formation in the classical citrate synthesis method derived from coupled in situ XANES and SAXS evaluation. J Am Chem Soc 132:1296–1301
35. Singh A (2012) Cucurbit[7]uril mediated viologen-fluorophore dyad for fluorescence off/on switch. Dissertation, University of Oklahoma
36. Gunawardana KB (2012) Study of Metal Enhanced Fluorescence of Dye-Doped silica Nanopartilces. Dissertation, University of Oklahoma
37. Liu X, Atwater M, Wang J, Huo Q (2007) Extinction coefficient of gold nanoparticles with different sizes and different capping ligands. Colloids Surf B: Biointerfaces 58(1):3–7
38. Near RD, Hayden SC, Hunter RE, Thackston D, El-Sayed MA (2013) Rapid and efficient prediction of optical extinction coefficients for gold nanospheres and gold nanorods. J Phys Chem C 117:23950–23955
39. Zhao Y, Pérez-Segarra W, Shi Q, Wei A., Dithiocarbamate assembly on gold. J. Am. Chem. Soc. 127 (20):7328
40. Park MH, Ofir Y, Samanta B, Arumugam P, Miranda OR, Rotello VM (2008) Nanoparticle immobilization on surfaces via activatable heterobifunctional dithiocarbamate bond formation. Adv Mater 20: 4185–4188
41. Gunawardana KB, Halterman RL (2011) Metal enhanced fluorescence of dye-doped silica nanoparticles. SWRM 898
42. Green NS, Gunawardana KB, Costello, WN, Halterman RL (2012) Metal enhanced fluorescence of dye-doped silica nanoparticles. SWRM 423
43. Vanderkooy A, Chen Y, Ferdinand G, Brook MA (2011) Silica shell/gold core nanoparticles: correlating shell thickness with the plasmonic red shift upon aggregation. ACS Appl Mater Interfaces 3:3942–3947
44. Halterman RL, Moore JL, Yip WT (2011) Cucurbit[7]uril disrupts aggregate formation between rhodamine B dyes covalently attached to glass substrates. J Fluoresc 21:1467–1478
45. Lazarides AA, Schatz GC (2000) DNA-linked metal nanosphere materials: structural basis for the optical properties. J Phys Chem B 104(3):460–467
46. Lakowicz JR (2005) Radiative decay engineering 5: metal-enhanced fluorescence and plasmon emission. Anal Biochem 337:171–194